# Targeting Axl favors an antitumorigenic microenvironment that enhances immunotherapy responses by decreasing Hif-1α levels

Marie-Anne Goyette[a,b], Islam E. Elkholi[a,b], Chloé Apcher[a,b], Hellen Kuasne[c], Carla V. Rothlin[d], William J. Muller[c], Darren E. Richard[e], Morag Park[c], Jean-Philippe Gratton[f], and Jean-François Côté[a,b,g,h,1]

[a]Cytoskeletal Organization and Cell Migration, Montreal Clinical Research Institute, Montréal, QC H2W 1R7, Canada; [b]Molecular Biology Programs, Université de Montréal, Montréal, QC H3T 1J4, Canada; [c]Rosalind and Morris Goodman Cancer Research Centre, McGill University, Montréal, QC H3A 1A1, Canada; [d]Department of Immunobiology and Pharmacology, School of Medicine, Yale University, New Haven, CT 06520; [e]Department of Molecular Biology, Medical Biochemistry and Pathology, Université Laval, Québec City, QC G1R 3S3, Canada; [f]Department of Pharmacology and Physiology, Université de Montréal, Montréal, QC H3C 3J7, Canada; [g]Department of Biochemistry and Molecular Medicine, Université de Montréal, Montréal, QC H3C 3J7, Canada; and [h]Department of Anatomy and Cell Biology, McGill University, Montréal, QC H3A 0C7, Canada

Edited by Joan S. Brugge, Harvard Medical School, Boston, MA, and approved May 1, 2021 (received for review November 19, 2020)

**Hypoxia is an important phenomenon in solid tumors that contributes to metastasis, tumor microenvironment (TME) deregulation, and resistance to therapies. The receptor tyrosine kinase AXL is an HIF target, but its roles during hypoxic stress leading to the TME deregulation are not well defined. We report here that the mammary gland–specific deletion of *Axl* in a HER2$^+$ mouse model of breast cancer leads to a normalization of the blood vessels, a proinflammatory TME, and a reduction of lung metastases by dampening the hypoxic response in tumor cells. During hypoxia, interfering with AXL reduces HIF-1α levels altering the hypoxic response leading to a reduction of hypoxia-induced epithelial-to-mesenchymal transition (EMT), invasion, and production of key cytokines for macrophages behaviors. These observations suggest that inhibition of Axl generates a suitable setting to increase immunotherapy. Accordingly, combining pharmacological inhibition of Axl with anti–PD-1 in a preclinical model of HER2$^+$ breast cancer reduces the primary tumor and metastatic burdens, suggesting a potential therapeutic approach to manage HER2$^+$ patients whose tumors present high hypoxic features.**

AXL | HER2 | hypoxia | tumor microenvironment | immunotherapy

Human Epidermal Growth Factor Receptor 2 (HER2) is overexpressed in about 20% of breast cancers, representing the HER2-positive (HER2$^+$) subtype that is associated with metastasis and poor prognosis (1, 2). While clinical success is partially achieved with the HER2-targeted therapies as a standard of care (e.g., Trastuzumab [Herceptin]), a significant pool of patients are either unresponsive or develop resistance to treatments. The development of new therapeutic approaches exploiting the tumor microenvironment (TME), like immunotherapy, is an attractive modality (3, 4). Indeed, combining immunotherapy and HER2-targeted agents is an emerging idea. Recently, clinical trials combined immune checkpoint point blockade (Pembrolizumab [anti–PD-1]) with Trastuzumab, but so far, it shows modest benefits (5). Indeed, there seems to be considerable roadblocks to hamper exploiting immunotherapies to treat HER2$^+$-resistant breast cancer patients. Thus, there is a need to better understand the immune environment of HER2 tumors to develop more effective therapeutic strategies (3). The TME and its associated stromal cells significantly influence therapy responses and affect the metastatic progression that causes the majority of cancer-related deaths (6, 7). Hypoxia is an integral component of the TME and is associated with a poor prognosis and increased risks of metastasis in various types of cancers, including breast cancer (8, 9). The adaptive response to hypoxia involves the up-regulation of a plethora of genes that are under the control of Hypoxia-inducible Factors (HIFs), and collectively, they contribute to angiogenesis, metabolic reprogramming, epithelial-to-mesenchymal transition (EMT), invasion, and immune evasion (10). In solid tumors, low oxygen ($O_2$) availability promotes cancer cell invasion, protumoral immune responses, and abnormal angiogenesis (8, 11, 12). In particular, the tumors' abnormal blood vessels are characterized by poor pericyte coverage and a noncontinuous basement membrane (BM) (13). This leads to dysfunctionalities such as poor perfusion and leakiness that accentuate hypoxia, facilitate tumor cell dissemination, and change the immune infiltration profiles (12, 14). Therefore, improving tumor blood vessel functionality, termed vessel normalization, has been suggested as a therapeutic goal (15). Consequently, targeting the TME appears as an interesting avenue to overcome resistance to cancer therapies including chemotherapy, radiotherapy, and immunotherapy (16–18).

AXL is a member of the TAM family of receptor tyrosine kinases that is composed of TYRO3, AXL, and MERTK. AXL is broadly expressed in various cancers in which it correlates with poor survival and increased risks of metastasis (19–22). More specifically, its expression in cancer cells supports the acquisition of mesenchymal features and provides advantages including cell invasion and resistance to drugs (19, 23, 24). In HER2$^+$ breast cancer cells, we previously reported a physical interaction between AXL and HER2 proteins that promoted invasion and metastasis

## Significance

**A significant pool of HER2$^+$ breast cancer patients are either unresponsive or become resistant to standards of care. New therapeutic approaches exploiting the tumor microenvironment, including immunotherapies, are attractive. Hypoxia shapes the tumor microenvironment toward therapy resistance and metastasis. Here, we report a role for AXL receptor tyrosine kinase in the hypoxic response by promoting HIF-1α expression. Interfering with Axl in a preclinical model of HER2$^+$ breast cancer normalizes the blood vessels and promotes a proinflammatory microenvironment that enhances immunotherapy response to reduce the primary and metastatic tumor burdens. Clinical trials so far suggest that achieving immunotherapy responses in HER2$^+$ cancers might be challenging, and our data might provide an important insight to circumvent a roadblock.**

Author contributions: M.-A.G., M.P., J.-P.G., and J.-F.C. designed research; M.-A.G., I.E.E., C.A., and H.K. performed research; C.V.R., W.J.M., and D.E.R. contributed new reagents/analytic tools; M.-A.G., I.E.E., C.A., H.K., and M.P. analyzed data; and M.-A.G., I.E.E., C.A., and J.-F.C. wrote the paper.

The authors declare no competing interest.

This article is a PNAS Direct Submission.



[1]To whom correspondence may be addressed. Email: jean-francois.cote@ircm.qc.ca.

This article contains supporting information online at https://www.pnas.org/lookup/suppl/doi:10.1073/pnas.2023868118/-/DCSupplemental.

Published July 15, 2021.

(20). Functionally, AXL expression correlated with the acquisition of EMT features and was linked to poor patients' outcome (20). Additionally, *AXL* has been described as a HIF target and has been shown to act with cMET to mediate the hypoxia-induced invasion of clear cell renal cell carcinoma (25). Nevertheless, the roles of AXL during hypoxic stress and in the TME deregulation remains poorly understood.

In this study, we aimed to directly test whether the TME of $HER2^+$ tumors can be harnessed toward a therapeutic strategy, more specifically, whether AXL inhibition may favor an immunotherapy response. We found that genetic deletion of *Axl* in the mammary epithelial cells in a $HER2^+$ breast cancer mouse model generated an antitumorigenic TME and reduced metastasis by altering the hypoxic response in tumor cells. Pharmacological inhibition of Axl then enhanced an anti–PD-1 immune checkpoint blockade as supported by reduced primary tumor and metastatic burdens. Collectively, these results indicate that targeting AXL during immunotherapy could be an innovative therapeutic strategy to improve the survival and quality of life of patients afflicted with $HER2^+$ cancers that are refractory to current treatments.

## Results

**Axl Contributes to the Deregulation of the TME in a Model of $HER2^+$ Breast Cancer.** *Axl* germline knockout (KO) mice were crossed with the $HER2^+$ breast cancer model that expresses an activated form of the HER2 rat ortholog in the mammary gland under the control of mouse mammary tumor virus (MMTV; NeuNDL2-5). This $Neu^+$ mouse model develops breast tumors that spontaneously metastasize to the lungs, and we previously reported that $Neu^+$:$Axl^{-/-}$ are protected from this metastatic progression without affecting primary tumor growth (20). Transcriptomic analyses of the *Axl*-null tumors 5 wks after tumor onset suggested a dampening of "hypoxia" and "angiogenesis" and an enhancement of "activation of immune response" by gene set enrichment analyses (GSEA) (Fig. 1 *A–C* and *SI Appendix*, Table S1). We hypothesized that the *Axl*-deficient tumors exhibit an antitumorigenic TME that can contribute to the poor capacity of those tumors to metastasize.

To address this, we collected the primary tumors 5 wks after the tumor onset to characterize their TME by immunostaining. $Neu^+$:$Axl^{-/-}$ tumors showed lower hypoxia levels as indicated by the decrease of the mean fluorescence intensity of two independent hypoxia markers, pimonidazole and GLUT-1 (Fig. 1*D* and *SI Appendix*, Fig. S1*A*). We next investigated the structural and functional changes in blood vessels and found that $Neu^+$:$Axl^{-/-}$ tumor blood vessels covered a larger area and had increased diameters when compared to control tumors (Fig. 1*E* and *SI Appendix*, Fig. S1*B*). They were less permeable, as suggested by a reduction of extravascular fibrinogen leakiness, and were better perfused, as demonstrated by intravenous injection of labeled Lectin (Fig. 1 *F* and *G*). The vessels also presented an increased coverage by $\alpha SMA^+$ pericytes and $Laminin^+$ basement membrane (BM) (Fig. 1 *H* and *I*). Thus, the decrease in intratumoral hypoxia and the vessel normalization observed could contribute to the reduction of metastasis observed in $Neu^+$:$Axl^{-/-}$ mice.

Moreover, $Neu^+$:$Axl^{-/-}$ tumors showed a differential immune cells profile compared to control tumors, as assessed by a flow cytometry analysis of a panel of lymphoid and myeloid markers (Fig. 1*J*). Interestingly, macrophages were less polarized toward an immune-suppressive phenotype ($CD206^+$) and also presented an increase in the expression of MHC class II (I-A/I-E), consistent with a proinflammatory activation state in the $Neu^+$:$Axl^{-/-}$ tumors (Fig. 1*J*). While $CD3^+$ lymphocytes were recruited into the tumor core, as shown by staining of tumor sections, no significant increase of this infiltration in $Neu^+$:$Axl^{-/-}$ tumors was observed (*SI Appendix*, Fig. S1*C*). Nevertheless, the difference of infiltration suggested a possible enhancement of antitumor response with an increase of natural killer (NK) cell activation (as measured by higher CD44 expression) and a significant reduction in the number of regulatory T cells (Treg) in $Neu^+$:$Axl^{-/-}$ tumors (Fig. 1*J*). Collectively, these results suggest that deleting Axl reduced the intratumoral hypoxia, normalized the blood vessels, and mediated a differential immune cells' representation in tumors.

**Conditional Deletion of Axl in the Mammary Epithelial Cells Generates an Antitumorigenic Microenvironment and Reduces the Metastatic Burden.** We next asked whether the effects of *Axl* KO were driven by *Axl* deletion in the tumor cells intrinsically or by its deletion in cells present in the microenvironment such as immune or endothelial cells. We generated primary tumor cell lines from $Neu^+$:$Axl^{+/+}$ and $Neu^+$:$Axl^{-/-}$ hosts and transplanted them into syngeneic wild-type FVB mice. Notably, RNA sequencing of $Neu^+$:$Axl^{-/-}$ tumor grafts recapitulated the gene expression signatures linked to the TME deregulation found initially in the tumors from $Neu^+$:$Axl^{-/-}$ mice (*SI Appendix*, Fig. S2 *A* and *B* and Table S2). $Neu^+$:$Axl^{-/-}$ tumor grafts also presented less hypoxia and produced blood vessels with a decreased permeability, increased perfusion, and increased pericytes and BM coverage (*SI Appendix*, Fig. S2 *C–I*). Thus, the normalized blood vessel phenotype could be reproduced when $Neu^+$:$Axl^{-/-}$ cells were grafted in a wild-type host, suggesting that this deregulation is a consequence of losing Axl in the cancer cells themselves. Furthermore, when investigating the immune profile of $Neu^+$:$Axl^{-/-}$ tumor grafts by flow cytometry, we found that macrophages were polarized toward a proinflammatory activation state ($CD206^-$, $I\text{-}A/I\text{-}E^+$), and there was a reduction in neutrophils compared to the controls (*SI Appendix*, Fig. S2*J*). These myeloid cells are known to regulate the TME by producing various inflammatory cytokines and proangiogenic factors, suggesting that Axl-expressing cancer cells could educate immune cells to contribute to the TME remodeling (26, 27). Thus, this experiment indicated that the TME changes observed in $Neu^+$:$Axl^{-/-}$ mice have been orchestrated by the cancer cells.

To confirm the cancer cell–autonomous role of Axl in the metastatic progression and the deregulation of the TME, *Axl* conditional KO mice were crossed with MMTV-NIC mice (MMTV-NeuNDL2-5-IRES-Cre) to obtain a specific deletion in the mammary epithelial cells (*SI Appendix*, Fig. S3*A*). Weekly monitoring of cohorts of $NIC^+$:$Axl^{wt/wt}$, $NIC^+$:$Axl^{wt/fx}$, and $NIC^+$:$Axl^{fx/fx}$ mice by palpation suggested no difference in tumor initiation (Fig. 2*A*). Moreover, there was no difference in the number of mammary intraepithelial neoplastic lesions 5 wks after tumor onset (*SI Appendix*, Fig. S3*B*). The tumor and metastatic burdens were also analyzed 5 wks after the appearance of the first mass. No difference in the total tumor weight per mouse was observed, and there were no significant changes in the proliferative and apoptotic status in the tumors (Ki67 or TUNEL, respectively) (Fig. 2*B* and *SI Appendix*, Fig. S3 *C* and *D*). Importantly, the loss of Axl altered the lung metastatic frequency and burden, as we observed in total *Axl* KO mice (20), suggesting a strong cancer cell–autonomous role in the phenotype (Fig. 2*C* and *SI Appendix*, Fig. S3*E*). Furthermore, the number of circulating tumor cells in the blood of the mice was reduced in $NIC^+$:$Axl^{wt/flx}$ and $NIC^+$:$Axl^{flx/flx}$ animals, suggesting that the cancer cells may be poorly invasive, as we have shown in ref. 20, and/or that the TME is unfavorable for intravasation (Fig. 2*D*). Thus, we decided to investigate whether the TME could also be rewired toward a tumor-suppressive phenotype in those tumors and consequently contribute to limit metastasis.

$NIC^+$:$Axl^{fx/fx}$ tumors displayed reduced hypoxia levels, and the blood vessels looked functionally normalized (Fig. 2 *E–I* and *SI Appendix*, Fig. S3 *F* and *G*). Similarly, vessels in $NIC^+$:$Axl^{fx/fx}$ tumors were less permeable, more perfused, and they presented a better pericyte and BM coverage as shown by immunostaining (Fig. 2 *E–I*). Furthermore, we investigated immune cell infiltration by flow cytometry to assess whether Axl deletion in the tumor cells could also generate a better immune response. Interestingly, macrophages and neutrophils were less present in $NIC^+$:$Axl^{fx/fx}$ tumors, and again, those macrophages showed a proinflammatory activation

state with less CD206 and more I-A/I-E expression (Fig. 2*J*). Moreover, $NIC^{+}$:$Axl^{fx/fx}$ tumor cells presented more $CD45^{+}$ immune cells with an increase of cytotoxic CD8 T cells and CD4 T cells (Fig. 2*J*). Globally, there was an increase in the recruitment of CD3+ lymphocytes in the core of $NIC^{+}$:$Axl^{fx/fx}$ tumors compared to the control (*SI Appendix*, Fig. S3*H*). Collectively, these data suggest that Axl expression in cancer cells contributes to deregulating the microenvironment to promote metastatic progression.

**AXL Is Required to Sustain HIF-1α Levels under Hypoxic Conditions.** We found that removing Axl in the cancer cells in vivo reduced the circulating tumor cells and metastasis. This could be explained by the reduction of hypoxia found in the $NIC^{+}$:$Axl^{-/-}$ tumors that could lead to a decrease of tumor cell invasion, normalized blood vessels, and increased immunosurveillance. Furthermore, we previously reported the interaction and crosstalk between AXL and HER2 to promote metastasis (20). This led us to explore their roles in hypoxic stress using tumor cell lines derived from the $NIC^{+}$:$Axl^{+/+}$ and $NIC^{+}$:$Axl^{-/-}$ mouse model, termed NIC WT (wild type) and *Axl* KO (knockout). Various receptor tyrosine kinases are known to regulate HIF complex levels and activity via different downstream pathways including PI3K/AKT, JAK/STAT3, and MAPK (28). For instance, HER2 regulates the synthesis of HIF-1α subunits by directly activating the PI3K/AKT/FRAP pathway (29).

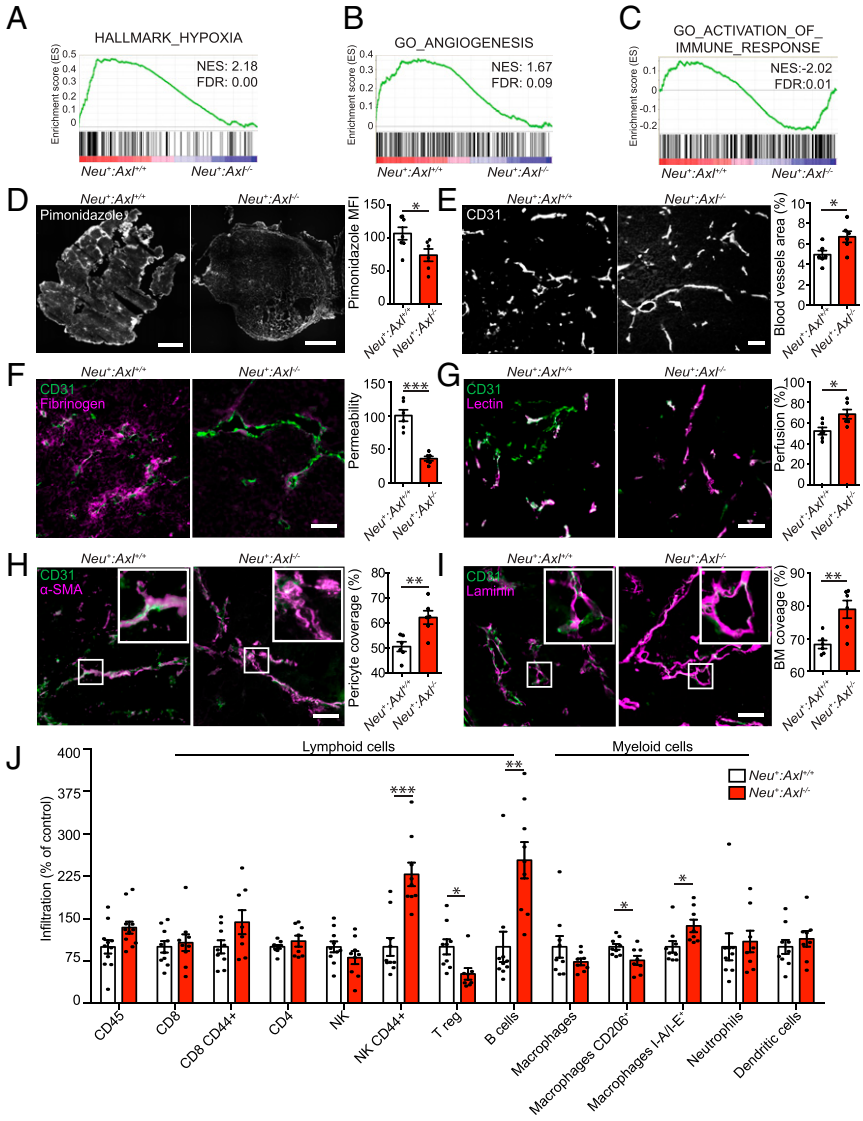


**Fig. 1.** Axl contributes to the TME deregulation. (*A*–*C*) GSEA of transcriptomic data (RNA-seq) of $Neu^{+}$:$Axl^{+/+}$ and $Neu^{+}$:$Axl^{-/-}$ tumors shows up-regulation of genes related to hypoxia (*A*) and angiogenesis (*B*) and a down-regulation of genes related to activation of immune response (*C*). (*D*) Pimonidazole staining reveals a reduction of hypoxia in $Neu^{+}$:$Axl^{-/-}$ tumors compared to control ($n = 7$ tumors, mean fluorescence intensity [MFI]) (Scale bars, 1 mm; $P = 0.0488$). (*E*) $Neu^{+}$:$Axl^{-/-}$ tumors present bigger blood vessels ($CD31^{+}$) with an increased total area ($n = 6$, $^{*}P = 0.0264$). (*F*) Reduced blood vessels permeability is observed in $Neu^{+}$:$Axl^{-/-}$ tumors with a decrease of Fibrinogen leakage in tumor tissue (Fibrinogen/CD31 ratio) ($n = 6$ tumors,$^{***}P < 0.0001$). (*G*) Intravenous injections of Rhodamine-labeled Lectin demonstrate a better perfusion of $Neu^{+}$:$Axl^{-/-}$ tumor blood vessels (Colocalization Lectin/ CD31) ($n = 6$ tumors, $^{*}P = 0.0168$). (*H*) Staining for CD31 and alpha Smooth Muscle Actin (αSMA) reveals a better pericyte coverage of blood vessels in $Neu^{+}$:$Axl^{-/-}$ tumors (Colocalization αSMA/CD31) ($n = 6$ tumors, $^{**}P = 0.0055$). (*I*) Staining for CD31 and Laminin shows more mature vessels with better BM coverage in $Neu^{+}$:$Axl^{-/-}$ tumors (Colocalization Laminin/CD31) ($n = 6$ tumors, $^{**}P = 0.0048$). (*J*) $Neu^{+}$:$Axl^{+/+}$ and $Neu^{+}$:$Axl^{-/-}$ tumors present differences in immune cells profile as shown by FACS analyses of a panel of lymphoid and myeloid markers ($n = 8$ to 12 tumors). NK cells ($CD3e^{-}NK1.1^{+}$) are more activated ($CD44^{+}$, $^{***}P = 0.0001$) in $Neu^{+}$:$Axl^{-/-}$ tumors, and those tumors present a decrease in regulatory T cells (Treg, $CD3e^{+}CD4^{+}CD25^{+}FoxP3^{+}$, $^{*}P = 0.0137$), an increase of B cells ($CD19^{+}B220^{+}$, $^{**}P = 0.0018$) and of macrophages ($F4/80^{+}$) expressing MHCII (I-A/I-$E^{+}$, $^{*}P = 0.0253$), and a decrease of macrophage expressing CD206 ($^{*}P = 0.0205$) in $Neu^{+}$:$Axl^{-/-}$ tumors. Data are presented as mean ± SEM. (Scale bars in E through I, 50 μm.)

Under hypoxic conditions (1% $O_2$ for 24h), *Axl* KO cells showed drastically reduced Her2 and Hif-1α protein levels when compared to control cells, while Hif-2α was not affected (Fig. 3*A*). Proteasome inhibition with MG132 rescued Her2 expression, suggesting a role for Axl in Her2 protein stability during hypoxia (*SI Appendix*, Fig. S4*A*). Therefore, Axl may modulate Hif-1α levels by regulating Her2 stability or by directly influencing hypoxic signaling pathways. HIF-1α subunit induction by hypoxia was also abrogated upon AXL depletion using small interfering RNA (siRNA) in human MCF10A cells stably expressing HER2, validating in another system the results observed in the mouse-derived cells (*SI Appendix*, Fig. S4*B*). Furthermore, in human $HER2^+$ breast cancer cells BT474 that do not express AXL, Axl overexpression potentiated HIF-1α induction and stabilized HER2 under hypoxia (Fig. 3*B*).

To demonstrate that Axl and Her2 activities are required for this effect, NIC WT cells were treated with Lapatinib (HER2 inhibitor) or R428 (AXL inhibitor). Single Her2 or Axl inhibition significantly decreased Hif-1α expression under hypoxia indicating that Her2 and Axl activity regulates Hif-1α levels under hypoxia in these cells. The combination of both inhibitors caused an additional reduction in Hif-1α levels, suggesting that Her2 and Axl can contribute independently to regulate Hif-1α expression during hypoxia (Fig. 3*C*). Furthermore, R428 decreased Her2 levels under hypoxia, confirming the role of Axl kinase activity on Her2 stability in hypoxic conditions (Fig. 3*C*). As expected, Her2 and Axl inhibition reduced pAkt levels, indicating that the Pi3k/Akt pathway could be implicated in the signaling of these receptors under hypoxia. We found that Pi3k inhibition with LY294002 also reduced Hif-1α levels in NIC WT cells (Fig. 3*D*). Thus, our results show that both Axl and Her2 can regulate Hif-1α levels under hypoxia potentially via activating the Pi3k/Akt pathway. Similar results were obtained in MCF10A-HER2 cells (*SI Appendix*, Fig. S4 *C* and *D*). To further dissect the contribution of AXL independently of HER2 signaling, triple-negative breast cancer cells expressing high levels of AXL, Hs578T, were used. The reduction of AXL levels using an siRNA decreased HIF-1α levels in hypoxia supporting a role for AXL independently of HER2 (Fig. 3*E*). Furthermore, ectopic expression of Axl in *Axl* KO cells rescued Her2 and Hif-1α expression (Fig. 3*F*). However, Hif-1α up-regulation was not completely lost by Lapatinib treatment, suggesting that Axl partially contributes to

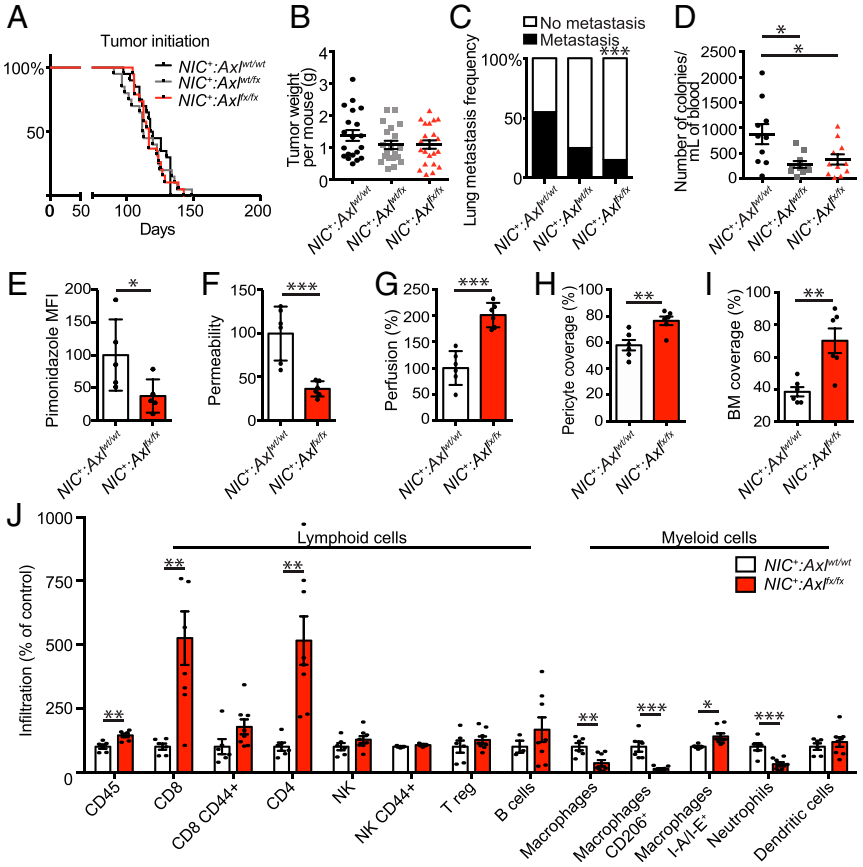


**Fig. 2.** Conditional *Axl* deletion in the mammary epithelial cells generates an antitumorigenic microenvironment and reduces the metastatic burden. (*A* and *B*) $NIC^+$:$Axl^{fx/fx}$ mice develop tumors at the same rate as control animals (*A*), and there is no difference in tumor mass (*B*) ($n = 20$ mice). (*C*) *Axl* deletion leads to a decrease of lung metastasis frequency ($n = 20$ mice, $^{***}P < 0.0001$). (*D*) Less circulating tumor cells are present in the blood of $NIC^+$:$Axl^{wt/fx}$ and $NIC^+$:$Axl^{fx/fx}$ mice compared to controls ($n = 10$ to 11 mice, $^{*}P = 0.0104$ and $^{*}P = 0.0324$). (*E*) A reduction of hypoxia in $NIC^+$:$Axl^{fx/fx}$ tumors compared to control is seen using pimonidazole staining ($n = 5$ tumors, $^{*}P = 0.0483$). (*F*) Fibrinogen staining in $NIC^+$:$Axl^{fx/fx}$ tumors reveals a diminution of tumor blood vessels permeability (Fibrinogen/CD31 ratio) ($n = 6$ tumors, $^{***}P = 0.0007$). (*G*) $NIC^+$:$Axl^{fx/fx}$ tumor blood vessels are more perfused by Rhodamine-labeled Lectin (Colocalization Lectin/ CD31) ($n = 6$ tumors, $^{***}P < 0.0001$). (*H*) A better pericyte coverage is observed in $NIC^+$:$Axl^{fx/fx}$ tumors blood vessels via staining with anti-CD31 and anti-αSMA antibodies (Colocalization αSMA/CD31) ($n = 6$ tumors, $^{**}P = 0.0048$). (*I*) Staining for CD31 and Laminin reveals more mature blood vessels with better BM coverage in $Neu^+$:$Axl^{-/-}$ tumors (Colocalization Laminin/CD31) ($n = 6$ tumors, $^{***}P = 0.0031$). (*J*) $NIC^+$:$Axl^{wt/wt}$ and $NIC^+$:$Axl^{fx/fx}$ tumors present differences in immune cells profile as shown by FACS analyses of a panel of lymphoid and myeloid markers ($n = 6$ to 8 tumors). $NIC^+$:$Axl^{fx/fx}$ tumors present a general increase of $CD45^+$ immune cells ($^{**}P = 0.0014$), an increase of CD8 and CD4 T cells ($CD3e^+CD8a^+$, $^{**}P = 0.0047$ and $CD3e^+CD4^+$, $^{**}P = 0.0029$), and a decrease of macrophages ($F4/80^+$, $^{**}P = 0.0054$) and neutrophils ($CD11b^+Ly6G^+$,$^{***}P = 0.0007$). Macrophages were also in a more proinflammatory activation state (CD206, $^{***}P = 0.0003$, I-A/I-E, $^{*}P = 0.0155$). Data are represented as mean ± SEM.


https://doi.org/10.1073/pnas.2023868118

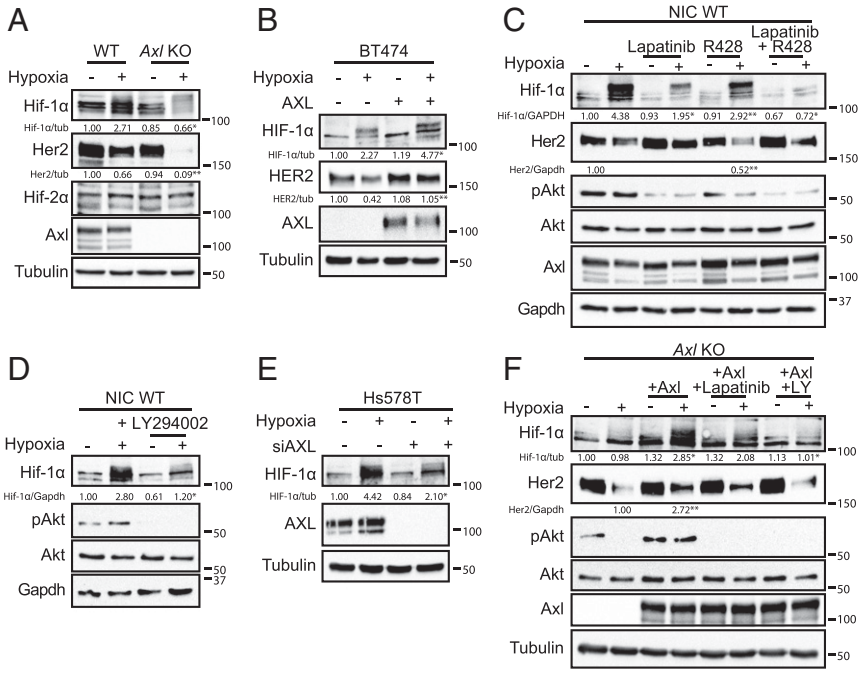


**Fig. 3.** Axl regulates HIF-1α levels in hypoxia. (*A*) *Axl* KO cells present a decrease of Hif-1α and Her2 protein levels when subjected to hypoxia (24 h, 1% $O_2$; the same hypoxic conditions are used throughout the figure) (*$P$ = 0.0282 and **$P$ = 0.0069, quantification from three independent experiments). (*B*) Axl overexpression in BT474 leads to an increase of HIF-1α and HER2 levels in hypoxia (*$P$ = 0.0166 and **$P$ = 0.0031, quantification from three independent experiments). (*C*) Inhibition of Axl (R428) or Her2 (Lapatinib) leads to a decrease of Hif-1α expression in NIC WT cells (*$P$ = 0.0225, **$P$ = 0.0027, *$P$ = 0.0255). A decrease of Her2 is also observed when cells are treated with R428 in hypoxia (**$P$ = 0.0026, quantification from three independent experiments). (*D*) Inhibition of Pi3k with LY294002 decreases Hif-1α levels in hypoxia in NIC WT cells (*$P$ = 0.0279, quantification from three independent experiments). (*E*) Reducing Axl expression in Hs578T cells reduced HIF-1α up-regulation in hypoxia (*$P$ = 0.0133, quantification from three independent experiments). (*F*) Axl overexpression in *Axl* KO cells increases Her2 expression in hypoxia (**$P$ = 0.0024) and rescues Hif-1α levels (*$P$ = 0.0348). Inhibition of Her2 or Pi3k decreases the rescue of Hif-1α levels (*$P$ = 0.0366, quantification from three independent experiments).

this up-regulation by stabilizing Her2 (Fig. 3*F*). Furthermore, LY294002 completely abrogated Axl-dependent HIF-1α up-regulation, indicating that Pi3k/Akt acts downstream of Axl to increase Hif-1α levels under hypoxic conditions (Fig. 3*F*). Remarkably, *AXL* expression in breast cancer patient samples from the TCGA-BRCA cohort correlated with *HIF-1α* gene expression independently of the subtype (*SI Appendix*, Fig. S4*E*). Taken together, these results indicate that Axl is required to ensure hypoxic Hif-1α expression by stabilizing Her2 and promoting Pi3k/Akt signaling. Hence, Axl can promote the deregulation of the TME and metastatic progression by regulating the Hif-1 complex during hypoxia.

**Axl Is Required for a Complete Hypoxic Response.** Since *Axl* KO cells reduced Hif-1α levels under hypoxia, *Axl* deletion could have an impact on the hypoxic transcriptome. To test this and to better understand the role of Axl in hypoxic adaptation required for TME remodeling and metastasis, we sequenced RNA isolated from NIC WT and *Axl* KO cells under 1% $O_2$. We conducted a gene ontology analysis of hypoxia–up-regulated genes that revealed that NIC WT cells showed an expected hypoxic response that includes the up-regulation of genes involved in migration, angiogenesis, and cytokine secretion. However, this response was reduced in *Axl* KO cells (Fig. 4*A* and *SI Appendix*, Fig. S5*A*). Overall, there were more up-regulated genes under hypoxia in NIC WT cells (Fig. 4*B*). The genes specifically up-regulated in *Axl* KO cells during hypoxia were linked to cell cycle, cellular metabolic process, cellular response to stress, and programmed cell death, suggesting a harder adaptation to hypoxia (*SI Appendix*, Fig. S5*B*). On the other hand, the Axl-dependent genes up-regulated under hypoxic conditions were principally associated with the processes mentioned in Fig. 4*A* but also specifically included the HIF-1α signaling pathway (Fig. 4*C*). Indeed, many HIF-1α target genes, mainly related to EMT, invasion, and immune evasion, were less expressed and/or differently modulated in the *Axl* KO compared to the WT cells (*SI Appendix*, Fig. S5*C*). This result suggests that Axl is essential for a complete hypoxic response. Therefore, these findings explain at least in part the changes in the TME and the reduced metastatic burden observed in our mouse models.

To investigate whether these observations can be clinically relevant, we analyzed the genes that correlate with *AXL* expression in breast cancer samples from METABRIC and TCGA breast cancer cohorts. In general, *AXL* correlated with the expression of genes linked to cell migration, inflammation, angiogenesis, and hypoxia, among others (*SI Appendix*, Fig. S5*D*). Interestingly, a significant proportion of the Axl-dependent genes induced under hypoxia and found in our RNA-seq analyses correlated with *AXL* expression in breast cancer patients (*SI Appendix*, Fig. S5*E*). These candidate genes were also related to processes linked to the TME and metastasis including response to $O_2$ levels, migration, angiogenesis, and inflammation, supporting a role for AXL in the hypoxic response and the TME deregulation in vivo (*SI Appendix*, Fig. S5*F*).

**Axl Is Essential for Hypoxia-Induced Changes that Drive Metastasis and TME Remodeling.** Hypoxia can promote metastatic progression by increasing tumor cell EMT and invasion via the up-regulation of EMT transcription factors that are themselves HIF targets (10, 11). In our RNA-seq experiment, *Snai2* and *Twist1* were found to be up-regulated under hypoxia in an Axl-dependent manner and correlated with *AXL* expression in human breast cancer samples (*SI Appendix*, Fig. S6 *A*–*C*). This led us to hypothesize that *Axl* deletion could decrease the ability of cells to become more mesenchymal in a hypoxic environment. Accordingly, the increase in the levels of the

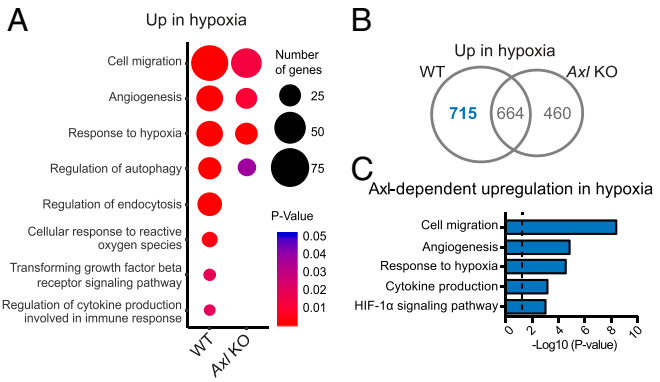


**Fig. 4.** Axl is required for a complete hypoxic response. RNA-seq analyses of NIC WT and *Axl* KO cells comparing gene modulation between normoxia and hypoxia conditions (72 h, 1% $O_2$). (*A*) Dot plot representing Gene Ontology (GO) analysis of up-regulated genes in hypoxia shows that *Axl* KO cells present lower genes related to hypoxia features. Circle sizes represent the number of genes associated with the GO, and the color represents the *P* value. (*B*) Venn diagram analysis of genes up-regulated in hypoxia in NIC WT and *Axl* KO cells. In blue are the genes that were used for the analysis in *C*. (*C*) GO analyses of the Axl-dependent up-regulated genes in hypoxia reveals genes linked to hypoxia-related features (in blue in *B*). Broken line indicates significance ($P = 0.05$).

mesenchymal marker Vimentin in NIC WT cells under hypoxic conditions was blunted in *Axl* KO cells, and this was rescued by re-expressing Axl (Fig. 5*A*). The same phenomenon was observed in human MCF10A-HER2 cells in which AXL levels were reduced by siRNA (*SI Appendix*, Fig. S6*D*). We next tested the role of AXL on hypoxia-induced cell motility. We found that hypoxia increased the invasion of NIC cells and MCF10A-HER2 cells in Boyden–Matrigel invasion assays (Fig. 5*B* and *SI Appendix*, Fig. S6*E*). In both cell lines, interfering with AXL by KO, siRNA, or R428 treatment reduced the basal invasion in normoxia and inhibited the promotion of invasion by hypoxia (Fig. 5*B* and *SI Appendix*, Fig. S6*E*). This was also reproduced in wound-healing assays in which AXL was required for hypoxia-induced cell migration (Fig. 5 *C* and *D* and *SI Appendix*, Fig. S6 *F* and *G*). These results demonstrate defects in hypoxia-induced EMT and invasion/migration when interfering with AXL. This further supports the notion that the ability of cancer cells to leave the primary site as circulating tumor cells and to form metastasis is impaired in $NIC^{+}$:$Axl^{fx/fx}$ mice.

Furthermore, cancer cells boost the production of different cytokines to remodel the TME and promote immune suppression under hypoxic conditions (10, 30). Interestingly, our RNA-seq data revealed that Axl removal affects the messenger RNA (mRNA) expression of some chemokines including *C-C Motif Chemokine Ligand 2* (*Ccl2*), *Colony-Stimulating Factor 1* (*Csf1*), *C-X-C Motif Chemokine Ligand*, and *2* (*Cxcl1* and *Cxcl2*) under hypoxia (*SI Appendix*, Fig. S7*A*). A cytokine profiling by a multiplex array was done to assess the secretion by WT and *Axl* KO cells of a variety of chemokines (*SI Appendix*, Table S3). Indeed, *Axl* KO cells secreted lower amounts of Ccl2, Csf1, Cxcl1, and Cxcl2 when subjected to hypoxic conditions (Fig. 6*A* and *SI Appendix*, Fig. S7 *B–D* and Table S3). Interestingly, among these candidates, *CCL2* expression correlated with *AXL* expression in human breast cancer, suggesting a possible clinical relevance of this finding (*SI Appendix*, Fig. S7*E*). CCL2 is a myeloid and lymphoid cell chemoattractant that promotes the recruitment of tumor-associated macrophages and affects their behavior in the TME (26, 31, 32). Tumor-associated macrophages are a major stromal component and can be reprogrammed by environmental signals into specialized subtypes including a spectrum of antitumoral (proinflammatory) or pro-tumoral (immune-suppressive or wound-healing) phenotypes (33–36). Importantly, we observed a reduction in macrophage numbers and polarization toward a protumoral phenotype in our *Axl* KO breast cancer mouse models (Fig. 1*J* and *SI Appendix*, Fig. S2*J*, and Fig. 2*J*). This infiltration was also validated by staining in the $NIC^{+}$:$Axl^{wt/wt}$ and $NIC$+:$Axl^{fx/fx}$ tumors (Fig. 6*B*). Furthermore, these infiltrated macrophages present a decrease of proliferation in *Axl*-null tumors as demonstrated by fluorescence-activated cell sorting (FACS) analysis of staining against phospho-Histone 3 (Fig. 6*C*). Therefore, we tested in vitro the requirement of Axl in tumor cells for macrophage proliferation, invasion, and polarization during hypoxia by treating bone marrow–derived macrophages with conditioned media (CM) from normoxic and hypoxic NIC WT and *Axl* KO cells. First, we observed that CM from hypoxic *Axl* KO cells was less efficient to promote the proliferation of macrophages (Fig. 6*D*). The addition of a neutralizing antibody against Ccl2 in WT CM also moderately reduced their proliferation, suggesting a partial implication of Ccl2 in this phenotype (Fig. 6*D*). Furthermore, CM from hypoxic NIC WT cells increased macrophage invasion compared to normoxic CM (Fig. 6*E*). However, CM from hypoxic *Axl* KO cells failed to stimulate invasion to the same extent, suggesting that *Axl* deletion in tumor cells can also affect the invasion and recruitment of macrophages in the tumor (Fig. 6*E*). In this case, we revealed a role for Ccl2 as shown by a reduction in invasion when an anti-Ccl2 antibody was added to the hypoxic WT CM (Fig. 6*E*). Finally, we investigated the effect of the hypoxic NIC CM on the polarization of bone marrow–derived macrophages. First, the immunosuppressive macrophage marker CD206 was less expressed in macrophages treated with hypoxic CM from *Axl* KO cells compared to control, correlating with in vivo observations (Fig. 6*F*). This phenotype was also partially recapitulated by the inhibition of Ccl2 (Fig. 6*F*). Moreover, macrophages treated with hypoxic *Axl* KO CM secreted less factors known to promote TME deregulation and angiogenesis such as Vegfa, Cxcl1, and Cxcl2 (Fig. 6 *G–I*). These results suggest that Axl is required for the secretion of factors, such as Ccl2, leading to macrophage proliferation, invasion, and polarization when cancer

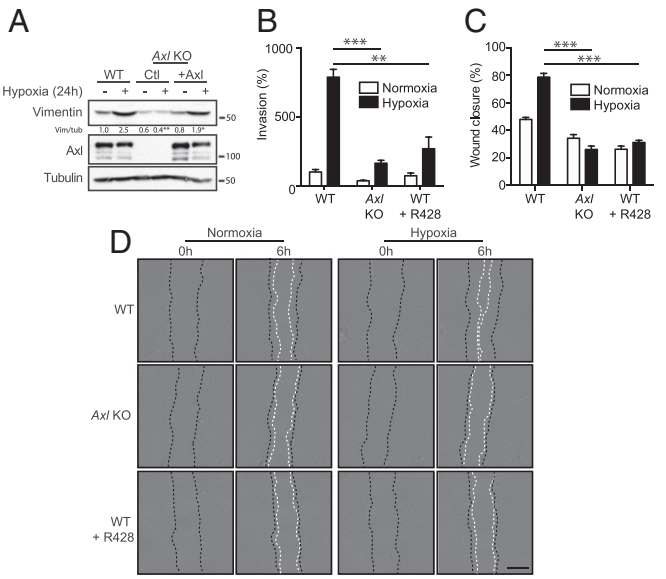


**Fig. 5.** *Axl* is required for hypoxia-induced EMT and cell migration and invasion. (*A*) In *Axl* KO cells, the mesenchymal marker Vimentin is not up-regulated in hypoxia (1% $O_2$, 24 h, $^{**}P = 0.0081$), and this is rescued by overexpressing Axl ($^{*}P = 0.0421$). (*B*) Hypoxia-induced cell invasion is reduced in *Axl* KO cells and in the presence of the AXL inhibitor R428 in a Boyden–Matrigel invasion assay ($^{***}P = 0.0005$, $^{**}P = 0.0070$). (*C* and *D*) Interfering with Axl reduces hypoxia-induced wound healing. The black lines represent the initial wounds, and the white lines indicate the migration fronts after 6 h ($P < 0.0001$). (Scale bar, 500 μm.) Data are represented as mean ± SEM.

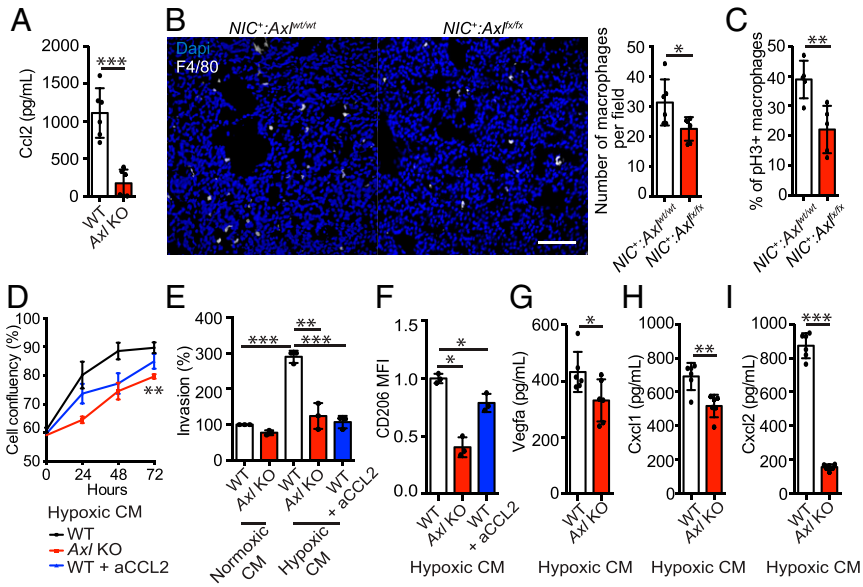


**Fig. 6.** Axl is required for hypoxia-induced secretion of factors that leads to macrophage proliferation, invasion, and polarization. (*A*) *Axl* KO cells secrete less Ccl2 in hypoxia compared to WT cells ($n = 6$, $^{***}P = 0.0001$). (*B*) Staining against F4/80 confirms the decrease of macrophages infiltration in $NIC^{+}$:$Axl^{fx/fx}$ tumors ($n = 6$ tumors, $^{*}P = 0.0313$). (Scale bars, 50 μm.) (*C*) Levels of phospho-Histone 3 (pH3) by FACS analyses shows less proliferation in infiltrated macrophages ($F4/80^{+}$) from $NIC^{+}$:$Axl^{fx/fx}$ tumors compared to $NIC^{+}$:$Axl^{wt/wt}$ tumors ($n = 6$ tumors, $^{**}P = 0.006$). (*D*) Hypoxic CM from *Axl* KO cells reduces the proliferation of bone marrow–derived macrophages compared to WT CM, as shown by an increase of cell confluency after 72 h ($^{**}P = 0.0081$). The addition of anti-Ccl2 in the WT CM also decreases partially this proliferation. (*E*) CM from hypoxic NIC cells induces the invasion of bone marrow–derived macrophages in a Boyden–Matrigel invasion assay, and Axl is required for this increase. Neutralizing Ccl2 in the hypoxic WT CM also decreases macrophages invasion ($n = 3$, $^{***}P < 0.0001$, $^{**}P = 0.0092$, and $^{***}P = 0.0002$). (*F*) The expression of CD206 is reduced in bone marrow–derived macrophages treated with hypoxic CM from *Axl* KO compared to CM from WT cells. Neutralizing Ccl2 also reduces CD206 expression ($n = 3$, $^{*}P = 0.0202$, $^{*}P = 0.0142$). (*G–I*) Macrophages treated with *Axl* KO hypoxic CM secrete less Vegfa, Cxcl1, and Cxcl2 ($n = 6$, $^{*}P = 0.0374$, $^{**}P = 0.0022$, and $^{***}P < 0.0001$).

cells are subjected to hypoxia. Consequently, this could affect their recruitment and reprogramming to promote angiogenesis and immune suppression to affect the TME and potentially the metastatic progression in our model of $HER2^{+}$ breast cancer.

**Axl Inhibition Generates an Antitumorigenic TME and Enhances Anti–PD-1 Immunotherapy Response.** Clinical trials so far suggest that achieving responses to immunotherapy in $HER2^{+}$ cancers is challenging (3, 4), and a better understanding of the $HER2^{+}$ TME may help to better classify possible responders. Indeed, there is a growing clinical need to define factors that modulate response to immunotherapies and specifically checkpoint inhibitors (3, 4, 37). The influence of hypoxia in the TME has been suggested to be one of those factors (38). As such, we chose to investigate the landscape of hypoxia among different molecular subtypes of breast cancer. Toward this goal, we performed a single-sample GSEA (ssGSEA). Hypoxia signatures scores, when applied to data from TCGA-BRCA, GSE58644, and METABRIC breast cancer samples (39–41), demonstrated that basal and $HER2^{+}$ subtypes present higher levels of hypoxia when compared to other breast cancer subtypes (Fig. 7 *A* and *B* and *SI Appendix*, Fig. S8 *A–D*). Additionally, $HER2^{+}$ patients whose tumors display higher hypoxia scores are associated with shorter overall and disease-free survival, suggesting that $HER2^{+}$ tumors with evidence of elevated signatures of hypoxia are more aggressive (Fig. 7*C* and *SI Appendix*, Fig. S8 *E–K*). In our experiments, hypoxic response elements, identified to be regulated by Axl, EMT, and tumor cell–macrophage interactions, can promote immune evasion and have been established as roadblocks to efficient immunotherapy (26, 42). Moreover, vascular normalization, as observed in $Neu^{+}$:$Axl^{-/-}$ and $NIC^{+}$:$Axl^{fx/fx}$ tumors, was demonstrated to enhance cancer immunotherapy (16, 43). Collectively, these observations suggest AXL as a druggable candidate to generate an improved setting for immunotherapy. This could be promising for $HER2^{+}$ patients that present prominent features of hypoxia.

Therefore, $Neu^{+}$ mice were treated individually and in combination with anti–PD-1 and AXL small-molecule inhibitor R428, as illustrated in *SI Appendix*, Fig. S9*A*. We observed that R428 treatment efficiently modulated the TME similarly to what we observed in total and conditional KO models. Indeed, there was a reduction of intratumoral hypoxia and a normalization of the blood vessels characterized by decreased permeability, increased perfusion, and improved pericyte coverage as shown by immunostaining (Fig. 7 *D–G*). Moreover, flow cytometry experiments showed that upon Axl inhibition, macrophages presented a proinflammatory activation state characterized by a reduction of CD206 and an increase of MCH-II (I-A/I-E) expression, confirming the effect of Axl inhibition on macrophage phenotype (Fig. 7*H*). Furthermore, on analyzing the tumor and metastatic burden of treated mice, we determined that $Neu^{+}$ mice were minimally responsive to anti–PD-1 therapy alone (Fig. 7 *I–K*). Only the combination of the anti–PD-1 immune checkpoint blockade and the Axl inhibitor was able to reduce the total tumor weight per mouse (Fig. 7*I*). Importantly, R428 treatment alone reduced the metastatic burden and frequency, as we reported previously (20), and the combination with anti–PD-1 potentiated this effect (Fig. 7 *J* and *K*). Interestingly, tumors treated with the combination of the two therapeutic agents presented an increase of CD8 T cells which, with the NK cells, were more activated ($CD44^{+}$), possibly explaining the effect of the combined therapy (Fig. 7*L*). Indeed, an increase in $CD3^{+}$-infiltrating cells was observed in the core of tumors cotreated with anti–PD-1 and R428 (*SI Appendix*, Fig. S9*B*). Furthermore, these tumors showed a significant increase in apoptosis but no difference in proliferation (*SI Appendix*, Fig. S9 *C* and *D*). These results suggest that AXL inhibition could be a powerful approach to generate an anti-tumorigenic microenvironment to improve immunotherapy and limit the metastatic spreading of breast cancer.

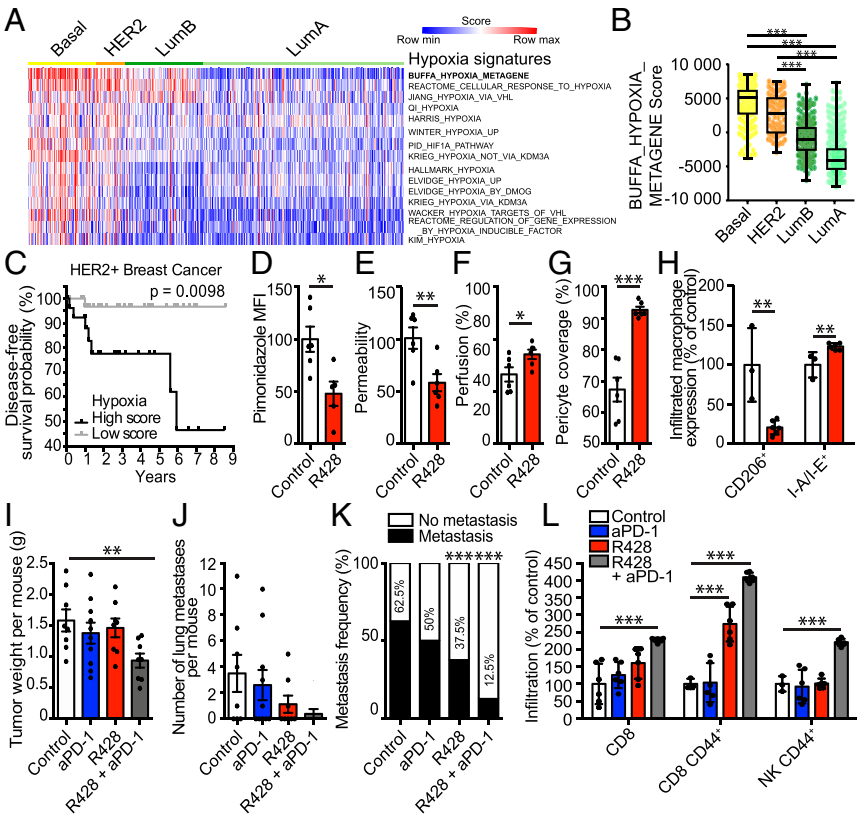


**Fig. 7.** Axl inhibition generates an antitumorigenic microenvironment that enhances anti–PD-1 therapy. (*A* and *B*) Heatmap of hypoxia signatures scores on TCGA breast cancer samples classified into distinct molecular subtypes based on gene expression profiling (Basal, HER2, Luminal A, and Luminal B). Basal and HER2$^+$ subtypes show higher hypoxia levels (***$P < 0.0001$). (*C*) The Kaplan–Meier curve of disease-free survival rate according to the hypoxia cluster indicates that HER2$^+$ cases with higher hypoxia scores present poorer outcomes. Refer to *SI Appendix*, Fig. S8*E* for related hierarchical clustering heatmap of HER2$^+$ patients ($n = 156$). (*D*) Treatment with R428 reduces intratumoral hypoxia as shown by pimonidazole staining ($n = 6$ tumors, *$P = 0.0135$). (*E*–*G*) Inhibition of Axl leads to a reduction of tumor blood vessel permeability (*E*, Fibrinogen/CD31 staining ratio, **$P = 0.0087$) and an increase of perfusion (*F*, Colocalization Lectin/ CD31 staining, *$P = 0.0412$) and pericyte coverage (*G*, Colocalization αSMA/ CD31 staining, ***$P < 0.0001$) ($n = 6$ tumors). (*H*) R428 treatment leads to the increase of proinflammatory activation state of tumor infiltrated macrophages (F4/80$^+$CD206$^+$, **$P = 0.0036$ and F4/80$^+$ I-A/I-E$^+$, **$P = 0.0096$) ($n = 3$ to 6 tumors). (*I*) The combination of Axl inhibition and anti–PD-1 immune checkpoint blockade reduces the primary tumor weight per mice ($n = 8$ to 10 tumors, **$P = 0.0085$). (*J* and *K*) The combination of R428 and anti–PD-1 further decreases the reduced metastatic burden (*J*, $P = 0.0525$) and frequency (*K*, ***$P = 0.0004$ and ***$P < 0.0001$) observed with R428 treatment alone ($n = 8$ to 10 tumors). (*L*) Combining R428 and anti–PD-1 increases the number of intratumoral CD8 T cells (CD3e$^+$CD8a$^+$, ***$P = 0.0004$) and increased their activity (CD3e$^+$CD8a$^+$CD44$^+$, ***$P = 0.0008$, and ***$P < 0.0001$) and the activity of NK cells (CD3e$^-$NK1.1$^+$CD44$^+$, ***$P < 0.0001$) ($n = 3$ to 6 tumors). Data are represented as mean ± SEM.

## Discussion

We previously reported the requirement of Axl in the metastatic progression of HER2$^+$ breast cancer where a total KO of *Axl* in the MMTV-Neu model leads to a drastic reduction of the metastatic burden without affecting primary tumor growth (20). AXL was required for the EMT and motility of HER2$^+$ cancer cells, suggesting that the reduction of invasive properties of AXL-depleted cancer cells leads to decreased metastasis. Here, we show that Axl also plays a role in the TME that impacts the metastatic progression. More specifically, *Axl* deletion in the mammary epithelium decreased the metastasis burden and generated an antitumorigenic TME by altering the hypoxic response in cancer cells. This reduced adaptation of *Axl* KO cancer cells to low $O_2$ levels resulted in decreased hypoxia-induced EMT, invasion, and macrophage-related cytokine production. Thus, interfering with Axl in a preclinical model of HER2$^+$ breast cancer generated an antitumorigenic TME that produced a suitable setting for immunotherapy and reduced the metastatic burden. Therefore, targeting AXL in the context of immunotherapy might be an interesting therapeutic strategy to treat HER2$^+$-resistant patients that present high hypoxic features.

It was previously reported that *AXL* is a direct HIF target and that its expression is up-regulated in clear cell renal cell carcinoma to promote invasion during hypoxia (25). This led to the notion that AXL is a hypoxia-induced protein that drives EMT, invasion, and eventually metastasis. However, AXL was not up-regulated in our HER2$^+$ breast cancer cell models during hypoxic stress. Interestingly, HIF-1α levels were reduced when AXL expression or activity was decreased, an effect that was further heightened upon hypoxia. During hypoxic stress, Axl was necessary for HIF-1α expression, and interfering with AXL led to an incomplete hypoxic response. This suggests that the AXL effect on HIF-1α expression can be accentuated in vivo in which low oxygen levels generate an adaptative response that has profound effects on the TME and metastasis. We propose a simple model where AXL acts on HIF-1α levels via HER2 stabilization and PI3K/AKT pathway, but more studies will be required to completely understand the mechanisms at play. Various RTKs can impinge on HIF levels by affecting its transcription, synthesis, or stability (28). The PI3K/AKT/FRAP pathway was shown to affect HIF-1α synthesis downstream of HER2 (29). Thus, this can also be happening downstream of AXL since we found that interfering with AXL in hypoxia reduced HER2 levels and AKT phosphorylation. Another possibility would be AXL regulating HIF-1α, either directly or indirectly at the transcriptional level. The latter possibility is supported by our RNA-seq data (*SI Appendix*, Fig. S5*C*), where *Hif-1α* mRNA levels were

lower in *Axl* KO cells during hypoxia compared to WT cells. Future investigations aiming at dissecting the AXL–HIF-1α connection would be of great significance.

We previously highlighted the crosstalk of AXL and HER2 leading to invasion, and we showed that the coupling of AXL to HER2 increased AXL stability and localization at the plasma membrane (20). The results in the current report suggest that the latter crosstalk might be extended to hypoxic conditions. Indeed, interfering with AXL in low-$O_2$ conditions reduced HER2 stability, thus possibly affecting the oncogenic signaling generated by HER2, including those leading to HIF-1α expression. To explore the roles of AXL in the hypoxic response, we took advantage of the differential transcriptome between *Axl* WT and *Axl* KO cells during hypoxic stress. Gene ontology analyses suggested a role for AXL in cell migration, angiogenesis, and cytokine production among many other processes linked to hypoxia. Consequently, we selected gene candidates whose expression correlated with AXL expression in human breast cancer samples and found that AXL was required for the induction of important EMT transcription factors (*Snai2* and *Twist1*) and key cytokines for macrophage function such as *Ccl2*. Thus, we showed that AXL was required for hypoxia-induced EMT and invasion. AXL is a well-established context-specific driver of EMT, and we previously showed in our model that AXL is required for TGF-β–induced EMT and cell invasion (20). This study showed that AXL is also required for EMT induction and invasion downstream of hypoxic stress, reinforcing the idea that AXL is a major player in these processes in various contexts. The roles of EMT in the metastatic progression are still debated (44, 45). Other than its role in tumor cell invasion, EMT could lead to chemoresistance and the secretion of cytokines that can affect the TME (42). For example, a positive feedback loop was shown between hypoxia, Snail expression, CXCL2/CXCL5-induced neutrophils recruitment, and impaired angiogenesis in tumors (46). This suggests that AXL's role as an EMT driver downstream of hypoxic stress can also be modulating the secretion of factors that affects the TME and thus leading to resistance to treatment and metastasis. Furthermore, the macrophage-related cytokine *Ccl2* was found down-regulated in *Axl* KO cells during hypoxia, and CM from these cells failed to enhance macrophage proliferation, invasion, and polarization. In vivo, macrophages are recruited to hypoxic areas of the tumor where their proangiogenic and anti-inflammatory phenotypes are refined (47, 48). Thus, the difference in immune profile and the normalization of the blood vessels observed in $NIC^{+}$:$Axl^{fx/fx}$ tumors could be explained by a reduction in macrophage-related cytokines production during hypoxia. Interestingly, the major angiogenic factor, *Vegfa*, was not differentially modulated in *Axl* KO cells during hypoxia (*SI Appendix*, Fig. S5*C* and Table S3). This further suggested that immune cells, including macrophages, may play an important role in the vessel normalization observed in $NIC^{+}$:$Axl^{fx/fx}$ tumors. In conclusion, the AXL depletion-mediated changes during the hypoxic response can collectively contribute to an antitumorigenic TME and to reduced metastatic burden in vivo.

Most patients afflicted with $HER2^{+}$ breast cancer are treated with targeted therapies against HER2 such as Trastuzumab, a drug-conjugated variant of Trastuzumab (T-DM1), or the kinase inhibitor Lapatinib. Unfortunately, some patients do not respond or develop resistance, and different avenues are being explored to overcome these challenges (49, 50). Our laboratory and others previously suggested that combining anti-HER2 and anti-AXL agents could be a good approach to enhance therapy and overcome resistance (20, 51). Furthermore, immunotherapy emerges as a powerful avenue to treat resistant and unresponsive patients, but so far, the PANCEA trial proposing the combination of anti–PD-1 and Trastuzumab offers modest improvements (3). This demonstrates the current clinical struggle of defining the group of patients that would benefit the most from anti–PD-1 therapy (37). The improvement of the TME, including reduced hypoxia, vascular normalization, and increased immune response, is a clinical goal to overcome resistance to various therapies, such as immunotherapy (16, 42, 52). Here, we show that basal and $HER2^{+}$ tumors present stronger signatures of hypoxia than other breast cancer subtypes, and these are associated with decreased survival in patients with $HER2^{+}$ tumors. Thus, targeting hypoxia in these tumors could be beneficial, and our experiments support that AXL inhibition could achieve this. AXL is an interesting druggable target because its loss or its inhibition appears to have no harmful effects in mice (20, 53). Thus, numerous clinical trials are ongoing with the AXL inhibitor R428 also known as BGB324 or Bemcentinib (54). Some trials are taking place in combination with immunotherapy, but only a few studies in preclinical models were done to support the possible efficiency of this combination (55, 56). Indeed, radiation and checkpoint immunotherapy-resistant PyMT tumors have been shown to overexpress Axl (56). In that study, Axl promotes an immune-suppressive microenvironment by reducing antigen presentation through MHC-I and enhancing immune-suppressive cytokine release. Therefore, low Axl-expressing clones respond better to immune checkpoint blockade (56). Furthermore, other studies link Axl/Pi3k signaling with increased expression of PD-L1 by tumor cells, and Axl inhibition potentiates PD-1 blockade in ID8 graft models (55, 57). Thus, we describe here an underlying mechanism and offer additional proof of concept for a combination of AXL and immune checkpoint inhibitors in a spontaneous preclinical cancer model. These notions also raise the question of AXL expression as a reliable predictor of response to immunotherapies in advanced HER2 breast cancer patients or other aggressive highly hypoxic basal breast cancers. Indeed, exploring such avenues might open the gate for potential therapeutic opportunities.

Collectively, our data demonstrate that anti-AXL therapy is sufficient to generate an antitumorigenic microenvironment and reduce metastasis in $HER2^{+}$ breast cancers by affecting the hypoxic response in cancer cells. This suggests a therapeutic opportunity in which targeting AXL in the context of immunotherapy in $HER2^{+}$-resistant patients could reduce the primary tumor and metastatic burdens.

## Materials and Methods

Animal experiments, tumor progression studies, quantification of circulating tumor cells, and orthotopic grafts are described in *SI Appendix, SI Materials and Methods*. Furthermore, detailed analysis of immunohistofluorescence, immunohistochemistry, and flow cytometry experiments, including the list of antibodies used, are described in *SI Appendix, SI Materials and Methods*. RNA sequencing, bioinformatics, and human data analyses details are also included in *SI Appendix, SI Materials and Methods*. Detailed information about cell lines, culture conditions, treatments, cell invasion assay, wound-healing assay, cytokine array, and proliferation assay were also described in *SI Appendix, SI Materials and Methods*. Statistical analyses were performed using unpaired Student *t* tests in which $P < 0.05$ is considered statistically significant, and more details are provided in *SI Appendix, SI Materials and Methods*.

**Data Availability.** RNA-seq data have been deposited in the Gene Expression Omnibus (GEO) (GSE158583).

**ACKNOWLEDGMENTS.** We thank Drs. Daniela Quail and Amélie Robert for critical reading of the manuscript. We also thank Dr. Tina Gruosso for generous expert advice on FACS protocols and analyses and Philippe P. Roux for the MCF10A-HER2 cells. We thank Suzie Riverin and IRCM mouse technicians for their assistance with mice, Dr. Dominic Filion for microscopy assistance, Simone Terouz for histology, Eric Massicotte and Julie Lord for FACS analyses, and Dr. Virginie Calderon for bioinformatic analysis of RNA-seq data. This work was supported by operating grants from the Canadian Institute of Health Research (CIHR) (MOP-142425 to J.-F.C. and J.-P.G.), CIHR Foundation (no. FDN-143281 to M.P.), Canadian Cancer Society (CCS no.: 706878 to M.P.), Reseau Cancer banque de tumeurs (Fonds de la Recherche du Québec en Santé (FRQS) and the Quebec Breast Cancer Foundation to M.P.), and the NIH (NIH-NCI R01 CA212376 to C.V.R.). J.-F.C. holds the Transat Chair in Breast Cancer Research. C.V.R. is a Howard Hughes Medical Institute Faculty Scholar. M.P. is a Distinguished James McGill Professor and holds the Diane and Sal Guerrera Chair in Cancer Genetics. M.-A.G. is a recipient of a CIHR Doctoral studentship. I.E.E. is a recipient of an FRQS Doctoral scholarship.

1. M. D. Seal, S. K. Chia, What is the difference between triple-negative and basal breast cancers? *Cancer J.* **16**, 12–16 (2010).
2. J. E. Visvader, Keeping abreast of the mammary epithelial hierarchy and breast tumorigenesis. *Genes Dev.* **23**, 2563–2577 (2009).
3. R. L. B. Costa, B. J. Czerniecki, Clinical development of immunotherapies for HER2$^+$ breast cancer: A review of HER2-directed monoclonal antibodies and beyond. *NPJ Breast Cancer* **6**, 10 (2020).
4. S. Adams *et al*., Current landscape of immunotherapy in breast cancer: A review. *JAMA Oncol.* **5**, 1205–1214 (2019).
5. S. Loi *et al*. and International Breast Cancer Study Group and the Breast International Group, Pembrolizumab plus trastuzumab in trastuzumab-resistant, advanced, HER2-positive breast cancer (PANACEA): A single-arm, multicentre, phase 1b-2 trial. *Lancet Oncol.* **20**, 371–382 (2019).
6. A. W. Lambert, D. R. Pattabiraman, R. A. Weinberg, Emerging biological principles of metastasis. *Cell* **168**, 670–691 (2017).
7. D. F. Quail, J. A. Joyce, Microenvironmental regulation of tumor progression and metastasis. *Nat. Med.* **19**, 1423–1437 (2013).
8. E. B. Rankin, J. M. Nam, A. J. Giaccia, Hypoxia: Signaling the metastatic cascade. *Trends Cancer* **2**, 295–304 (2016).
9. M. Schindl *et al*., Overexpression of hypoxia-inducible factor 1alpha is associated with an unfavorable prognosis in lymph node-positive breast cancer. *Clin. Cancer Res* **8**, 1831–1837 (2002).
10. L. Schito, G. L. Semenza, Hypoxia-inducible factors: Master regulators of cancer progression. *Trends Cancer* **2**, 758–770 (2016).
11. E. B. Rankin, A. J. Giaccia, Hypoxic control of metastasis. *Science* **352**, 175–180 (2016).
12. P. Carmeliet, R. K. Jain, Principles and mechanisms of vessel normalization for cancer and other angiogenic diseases. *Nat. Rev. Drug Discov.* **10**, 417–427 (2011).
13. S. Morikawa *et al*., Abnormalities in pericytes on blood vessels and endothelial sprouts in tumors. *Am. J. Pathol.* **160**, 985–1000 (2002).
14. L. L. Munn, R. K. Jain, Vascular regulation of antitumor immunity. *Science* **365**, 544–545 (2019).
15. S. Goel *et al*., Normalization of the vasculature for treatment of cancer and other diseases. *Physiol. Rev.* **91**, 1071–1121 (2011).
16. Y. Huang *et al*., Improving immune-vascular crosstalk for cancer immunotherapy. *Nat. Rev. Immunol.* **18**, 195–203 (2018).
17. X. Jing *et al*., Role of hypoxia in cancer therapy by regulating the tumor microenvironment. *Mol. Cancer* **18**, 157 (2019).
18. K. C. Valkenburg, A. E. de Groot, K. J. Pienta, Targeting the tumour stroma to improve cancer therapy. *Nat. Rev. Clin. Oncol.* **15**, 366–381 (2018).
19. C. Gjerdrum *et al*., Axl is an essential epithelial-to-mesenchymal transition-induced regulator of breast cancer metastasis and patient survival. *Proc. Natl. Acad. Sci. U.S.A.* **107**, 1124–1129 (2010).
20. M. A. Goyette *et al*., The receptor tyrosine kinase AXL is required at multiple steps of the metastatic cascade during HER2-positive breast cancer progression. *Cell Rep.* **23**, 1476–1490 (2018).
21. L. Lozneanu *et al*., Computational and immunohistochemical analyses highlight AXL as a potential prognostic marker for ovarian cancer patients. *Anticancer Res.* **36**, 4155–4163 (2016).
22. E. B. Rankin *et al*., AXL is an essential factor and therapeutic target for metastatic ovarian cancer. *Cancer Res.* **70**, 7570–7579 (2010).
23. K. Vuoriluoto *et al*., Vimentin regulates EMT induction by slug and oncogenic H-Ras and migration by governing AXL expression in breast cancer. *Oncogene* **30**, 1436–1448 (2011).
24. M. K. Asiedu *et al*., AXL induces epithelial-to-mesenchymal transition and regulates the function of breast cancer stem cells. *Oncogene* **33**, 1316–1324 (2014).
25. E. B. Rankin *et al*., Direct regulation of GAS6/AXL signaling by HIF promotes renal metastasis through SRC and MET. *Proc. Natl. Acad. Sci. U.S.A.* **111**, 13373–13378 (2014).
26. D. G. DeNardo, B. Ruffell, Macrophages as regulators of tumour immunity and immunotherapy. *Nat. Rev. Immunol.* **19**, 369–382 (2019).
27. C. Murdoch, M. Muthana, S. B. Coffelt, C. E. Lewis, The role of myeloid cells in the promotion of tumour angiogenesis. *Nat. Rev. Cancer* **8**, 618–631 (2008).
28. A. A. Glück, D. M. Aebersold, Y. Zimmer, M. Medová, Interplay between receptor tyrosine kinases and hypoxia signaling in cancer. *Int. J. Biochem. Cell Biol.* **62**, 101–114 (2015).
29. E. Laughner, P. Taghavi, K. Chiles, P. C. Mahon, G. L. Semenza, HER2 (neu) signaling increases the rate of hypoxia-inducible factor 1alpha (HIF-1alpha) synthesis: Novel mechanism for HIF-1-mediated vascular endothelial growth factor expression. *Mol. Cell. Biol.* **21**, 3995–4004 (2001).
30. V. Petrova, M. Annicchiarico-Petruzzelli, G. Melino, I. Amelio, The hypoxic tumour microenvironment. *Oncogenesis* **7**, 10 (2018).
31. E. N. Arwert *et al*., A unidirectional transition from migratory to perivascular macrophage is required for tumor cell intravasation. *Cell Rep.* **23**, 1239–1248 (2018).
32. M. Gschwandtner, R. Derler, K. S. Midwood, More than just attractive: How CCL2 influences myeloid cell behavior beyond chemotaxis. *Front. Immunol.* **10**, 2759 (2019).
33. B. Z. Qian, J. W. Pollard, Macrophage diversity enhances tumor progression and metastasis. *Cell* **141**, 39–51 (2010).
34. M. Yang, D. McKay, J. W. Pollard, C. E. Lewis, Diverse functions of macrophages in different tumor microenvironments. *Cancer Res.* **78**, 5492–5503 (2018).
35. R. A. Franklin *et al*., The cellular and molecular origin of tumor-associated macrophages. *Science* **344**, 921–925 (2014).
36. M. De Palma, C. E. Lewis, Macrophage regulation of tumor responses to anticancer therapies. *Cancer Cell* **23**, 277–286 (2013).
37. D. B. Doroshow *et al*., PD-L1 as a biomarker of response to immune-checkpoint inhibitors. *Nat. Rev. Clin. Oncol.* **18**, 345–362 (2021).
38. M. Z. Noman *et al*., Improving cancer immunotherapy by targeting the hypoxic tumor microenvironment: New opportunities and challenges. *Cells* **8**, E1083 (2019).
39. D. C. Koboldt *et al*. and Cancer Genome Atlas Network, Comprehensive molecular portraits of human breast tumours. *Nature* **490**, 61–70 (2012).
40. C. Curtis *et al*. and METABRIC Group, The genomic and transcriptomic architecture of 2,000 breast tumours reveals novel subgroups. *Nature* **486**, 346–352 (2012).
41. A. Tofigh *et al*., The prognostic ease and difficulty of invasive breast carcinoma. *Cell Rep.* **9**, 129–142 (2014).
42. L. A. Horn, K. Fousek, C. Palena, Tumor plasticity and resistance to immunotherapy. *Trends Cancer* **6**, 432–441 (2020).
43. Y. Huang, S. Goel, D. G. Duda, D. Fukumura, R. K. Jain, Vascular normalization as an emerging strategy to enhance cancer immunotherapy. *Cancer Res.* **73**, 2943–2948 (2013).
44. K. R. Fischer *et al*., Epithelial-to-mesenchymal transition is not required for lung metastasis but contributes to chemoresistance. *Nature* **527**, 472–476 (2015).
45. X. Zheng *et al*., Epithelial-to-mesenchymal transition is dispensable for metastasis but induces chemoresistance in pancreatic cancer. *Nature* **527**, 525–530 (2015).
46. J. Faget *et al*., Neutrophils and snail orchestrate the establishment of a pro-tumor microenvironment in lung cancer. *Cell Rep.* **21**, 3190–3204 (2017).
47. D. Laoui *et al*., Tumor hypoxia does not drive differentiation of tumor-associated macrophages but rather fine-tunes the M2-like macrophage population. *Cancer Res.* **74**, 24–30 (2014).
48. A. Casazza *et al*., Impeding macrophage entry into hypoxic tumor areas by Sema3A/Nrp1 signaling blockade inhibits angiogenesis and restores antitumor immunity. *Cancer Cell* **24**, 695–709 (2013).
49. M. De Laurentiis *et al*. Targeting HER2 as a therapeutic strategy for breast cancer: A paradigmatic shift of drug development in oncology. *Ann. Oncol. Off. J. Eur. Soc. Medical Oncol. / ESMO* **16** (Suppl. 4), iv7-13 (2005).
50. T. Mukohara, Mechanisms of resistance to anti-human epidermal growth factor receptor 2 agents in breast cancer. *Cancer Sci.* **102**, 1–8 (2011).
51. L. Liu *et al*., Novel mechanism of lapatinib resistance in HER2-positive breast tumor cells: Activation of AXL. *Cancer Res.* **69**, 6871–6878 (2009).
52. P. Sharma, S. Hu-Lieskovan, J. A. Wargo, A. Ribas, Primary, adaptive, and acquired resistance to cancer immunotherapy. *Cell* **168**, 707–723 (2017).
53. Q. Lu *et al*., Tyro-3 family receptors are essential regulators of mammalian spermatogenesis. *Nature* **398**, 723–728 (1999).
54. ClinicalTrials.gov, BGB324, R428 or bemcentinib in clinical trials. https://clinicaltrials.gov/ct2/results?term=bgb324+OR+r428&Search=Clear&age_v=&gndr=&type=&rslt=. Accessed 12 November 2020.
55. Z. Guo, Y. Li, D. Zhang, J. Ma, Axl inhibition induces the antitumor immune response which can be further potentiated by PD-1 blockade in the mouse cancer models. *Oncotarget* **8**, 89761–89774 (2017).
56. T. A. Aguilera *et al*., Reprogramming the immunological microenvironment through radiation and targeting Axl. *Nat. Commun.* **7**, 13898 (2016).
57. H.D. Skinner *et al*. Integrative analysis identifies a novel AXL-PI3 kinase-PD-L1 signaling axis associated with radiation resistance in head and neck cancer. *Clin. Cancer Res.* **23**, 2713–2722 (2017).